CHAPTER III
RESULTS AND DISSCUSSION

In this chapter, we present and discuss the results in two parts: those on the binary systems and those on the ternary systems. The binary systems consist of the aqueous polymer solutions and the aqueous surfactant solutions and the ternary solutions are the aqueous polymer-surfactant solutions. Because the polymer and the surfactant each has unique properties, the mixtures of polymer and surfactant will be expected to display features that are not present in the binary system alone so a study of the binary system is a necessary prerequisite and provides baseline data for a better appreciation and understanding of the ternary polymer-surfactant solutions.

3.1 Binary Systems

3.1.1 The HPC/Water System

The molecular characterization of hydroxypropylcellulose was carried out using viscosity, dynamic light scattering, static light scattering, and gel permeation chromatography (GPC) measurements.

From viscosity measurement, the intrinsic viscosity ($[\eta]$) of HPC at 30 °C was determined using the Kraemer and the Huggins plots as shown in Figure 3.1. Both plots give the same value of the intrinsic viscosity within experimental error which is 0.132 l/g. It is noted that the inverse intrinsic viscosity ($[\eta]^{-1}$) provides a useful measure of the overlap concentration (c^*) which is the concentration where the solution concentration is approximately equal to the average concentration of segments with the domain of a single coil.

Above this concentration, the polymer solution emerges into semidilute regime. The overlap concentration of this HPC solution is therefore 7.6 g/l.

$$c^* = 1/[\eta] \qquad (3.1)$$

Figure 3.2 shows data on the concentration dependence of the relative viscosity (η_r) for the HPC solutions extending into the semidilute region. These data show a nonlinear in concentration dependence of the relative viscosity in the semidilute regime due to entanglement interactions between chains.

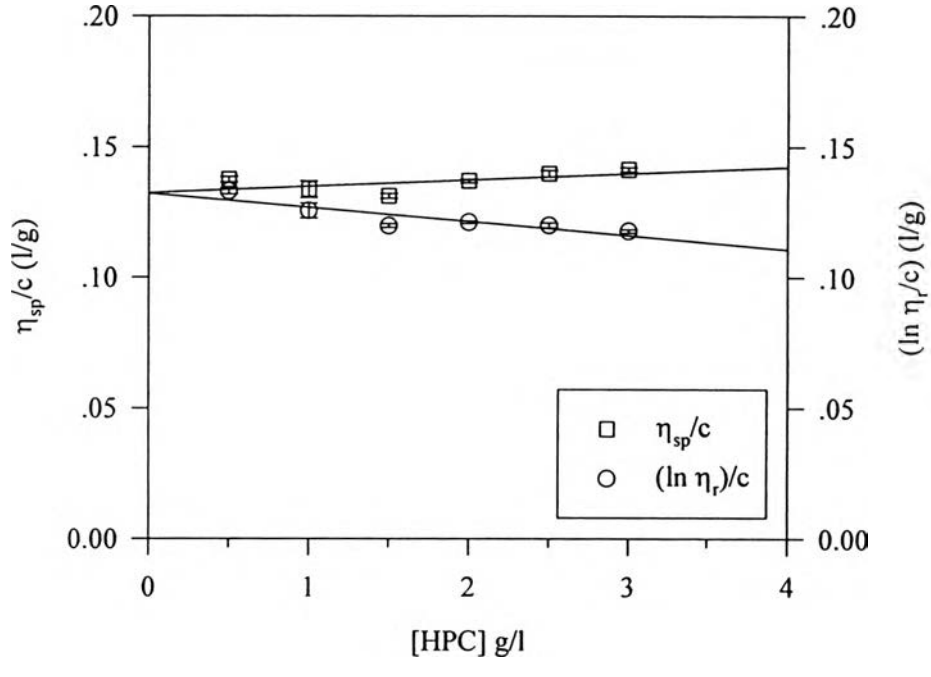

Figure 3.1 Plot of the reduced viscosity (η_{sp}/c) and the inherent viscosity ($\ln \eta_r/c$) as a function of total HPC concentration at 30 °C for the HPC/water system.

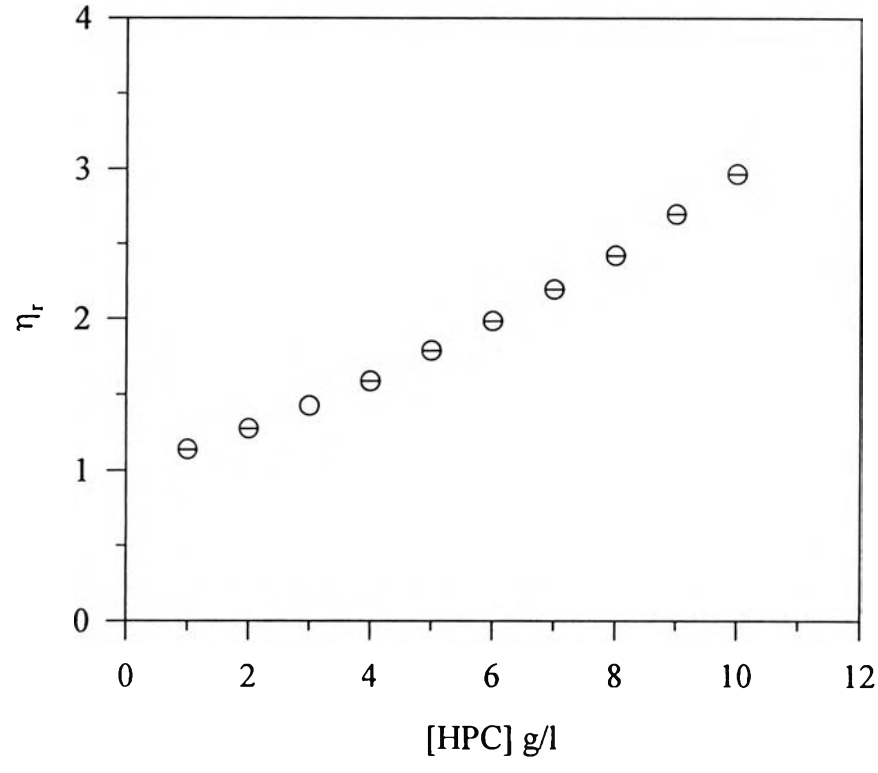

Figure 3.2 Plot of the relative viscosity (η_r) as a function of total HPC concentration at 30 °C for the HPC/water system extending to semidilute regime.

Figure 3.3a shows the apparent diffusion coefficient as a function of the scattering vector (q) for the fixed HPC concentration of 1 g/l. Different scattering vector values come from varying the angle (Eq. 3.2). When the apparent diffusion coefficient is extrapolated to zero angle, we get the diffusion coefficient D_c which is the center of mass diffusion for a given HPC concentration. Figure 3.3b shows the diffusion coefficient for HPC as a function of HPC concentration at 30 °C. The HPC concentrations were in the dilute concentration range, $c < c^*$. An approximate value for the hydrodynamic radius (R_h) can be obtained by extrapolating the data in Figure 3.3b to infinite

dilution and the hydrodynamic radius was calculated using the *Stokes-Einstein* equation (Eq. 3.3). This gives a hydrodynamic radius of 18.9 nm for the hydroxypropylcellulose sample at 30 °C.

$$q = (4\pi n/\lambda) \sin(\theta/2) \qquad (3.2)$$

where q = the scattering vector
n = the solvent refractive index
λ = the wavelength
θ = the angle

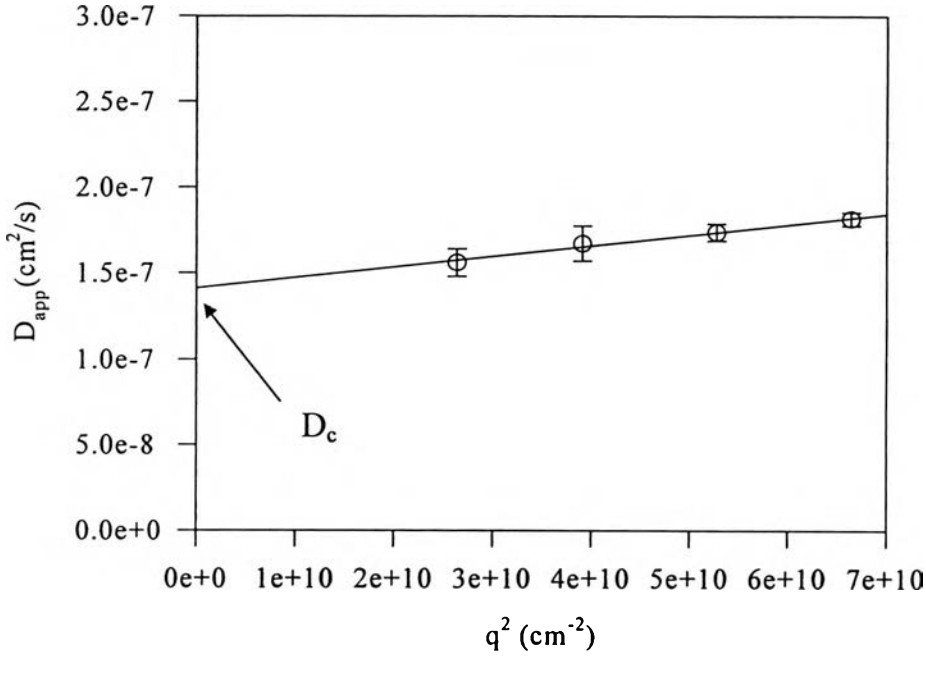

Figure 3.3a Plot of the apparent diffusion coefficient as a function of the scattering vector at 30 °C at the fixed HPC concentration of 1 g/l.

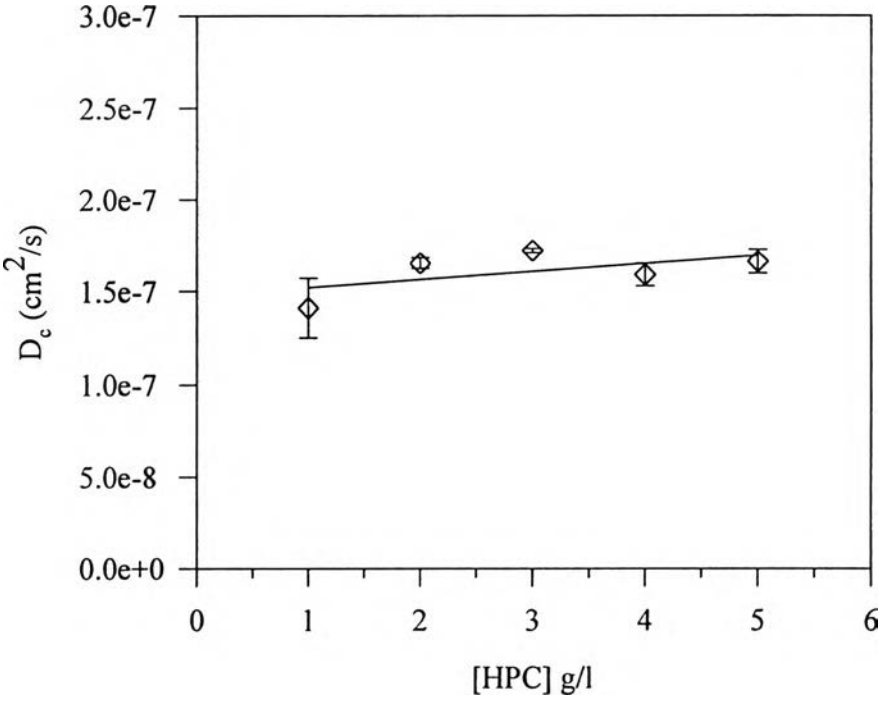

Figure 3.3b Plot of the diffusion coefficient as a function of total HPC concentration at 30 °C for the HPC/water system.

$$R_h = k_B T/6\pi\eta_o D_o \qquad (3.3)$$

where k_B = the Boltzman constant

η_o = the solvent viscosity

T = the temperature (K)

Conventionally, the concentration dependence of the diffusion coefficient in binary polymer dilute solution is given by

$$D = D_o (1 + k_D c + \ldots) \qquad (3.4)$$

where k_D is related to the second virial coefficient, i.e., to the pair interaction potential, by

$$k_D = 2A_2M - k_f - 2v_2 \quad (3.5)$$

where k_f describes the concentration dependence of the friction factor and v_2 is the partial specific volume of the particle. k_D is the sum of a static factor which is proportional to the second virial coefficient, A_2, and the concentration dependence of the friction coefficient. Thus k_D is another measure of the quality of a solvent for a solvent and a polymer pair; it is generally positive in good solvents and zero and negative in weaker solvent. In this study, k_D of HPC is equal to 30.0 $cm^3\ g^{-1}$ so it indicates that water is a good solvent for HPC.

For the static light scattering, the weight-average molecular weight (M_w), the radius of gyration (R_g), and the second virial coefficient (A_2) calculated by Zimm plot are shown in Table 3.1.

Table 3.1 Solution properties of HPC in water

M_w (g/mol)	R_g (nm)	A_2 ($cm^3\ mol\ g^{-1}$)	D_o ($cm^2\ s^{-1}$)	R_h (nm)	$[\eta]$ (l/g)
58124	49.5	0.003	1.474×10^{-7}	18.9	0.132

Figure 3.4 shows a GPC chromatogram of HPC. The results are shown in Table 3.2, measured using polystyrene standard.

Table 3.2 Summary for GPC results

Retention time (min)	M_n (g/mol)	M_w (g/mol)	M_z (g/mol)	Polydispersity
15.583	32193	81519	144971	2.522883

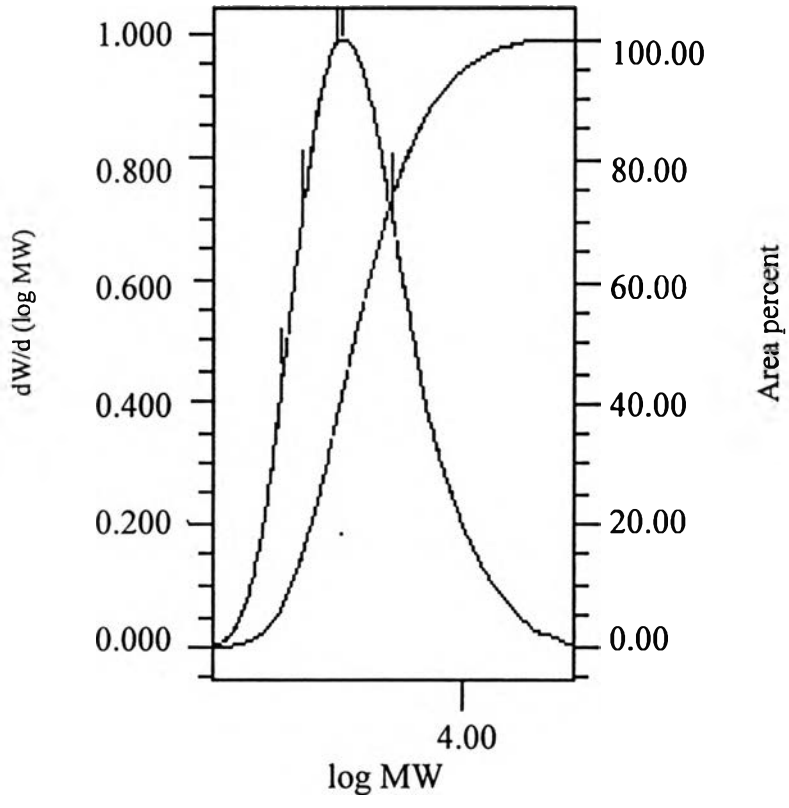

Figure 3.4 A GPC chromatogram of hydroxypropylcellulose at 25 °C.

3.1.2 The OTG/Water System

The critical micelle concentration (CMC) for OTG was measured using the surface tension method. The onset of micellization can be determined from a surface tension versus concentration plot which shows a sharp break at the CMC followed by an almost constant surface tension with increase in surfactant concentration.

The surface tension change comes from the fact that when surfactants are dissolved in water, materials that contain a hydrophobic group distort the structure of the water and therefore increase the free energy of the system. They therefore concentrate to reside at the surface, where, by orienting so that their hydrophobic groups are directed away from the solvent, the free energy of the solution is minimized. However, there is another means of

minimizing the free energy in these systems. The distortion of the solvent structure can also be decreased (and the free energy of the solution reduced) by the aggregation of the surfactant molecules into clusters (micelle) with their hydrophobic groups oriented toward the solvent. Micellization is therefore an alternative mechanism to adsorption at the interface by removing hydrophobic groups from contact with water, thereby reducing the free energy of the system (Rosen, 1989).

The CMC value of OTG in water is equal to 8.50 mM which is in agreement with those reported in the literature (Table 3.3).

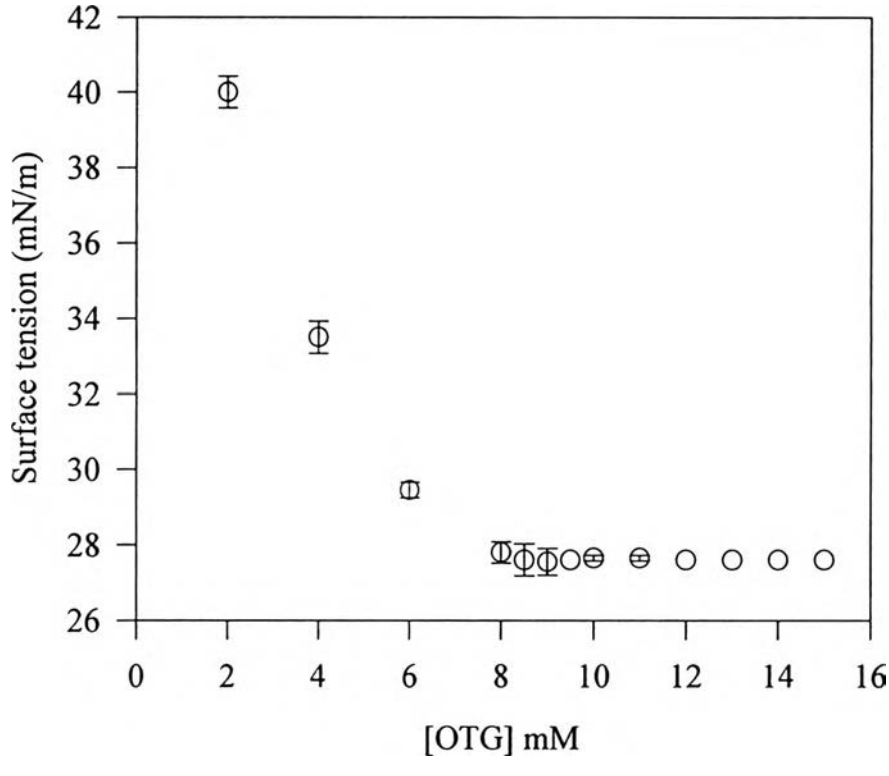

Figure 3.5 Plot of surface tension as a function of total OTG concentration at 30 °C for the OTG/water system.

Table 3.3 Literature data on the CMC values of OTG

T (°C)	CMC (mM)	Methods	References
20	10.1	Pyrene fluorescence method	Brackman *et al.*, 1988
25	8.05	Microcalorimetric method	Brackman *et al.*, 1988
25	8.7	Pyrene fluorescence method	Brackman *et al.*, 1988
25	9.2	Bromophenolblue absorption method	Brackman *et al.*, 1988
a	9.0	Ross & Oliver method	Sailto and Tsuchiya, 1984
25	9.0	Pyrene fluorescence method	Winnik, 1990

[a] Data not available

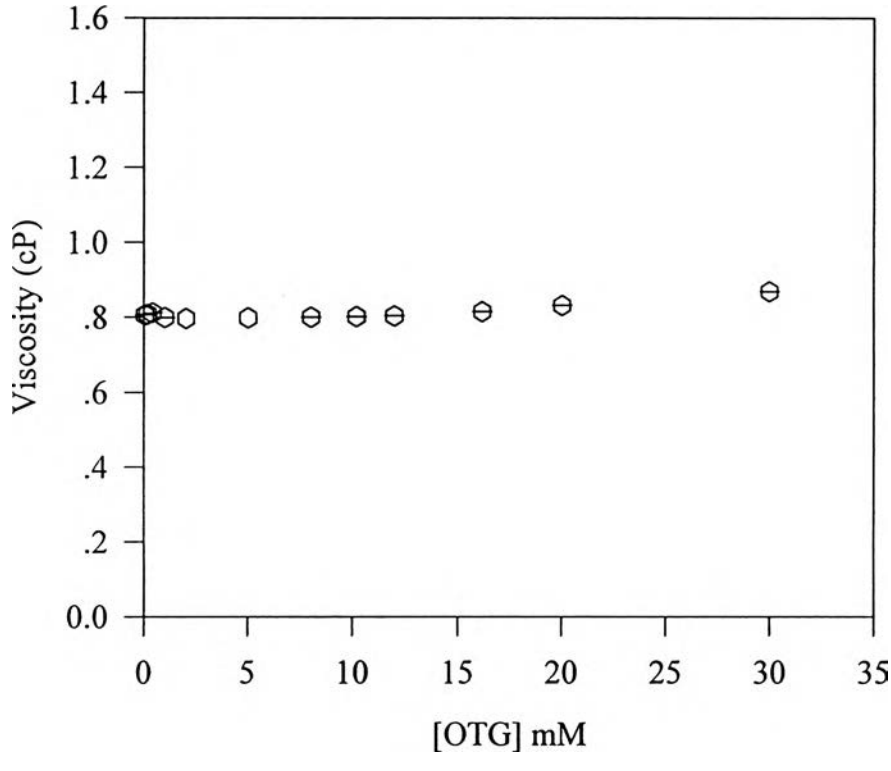

Figure 3.6 Plot of the viscosity as a function of total OTG concentration at 30 °C for the OTG/water system.

Figure 3.6 shows the viscosity of OTG as a function of OTG concentration. From this Figure, the viscosity of OTG slightly increases with increase of OTG concentration up to about seven times of the normal CMC value.

3.1.3 The CTAB/Water System

The critical micelle concentration of CTAB was determined by both surface tension and conductivity measurements as shown in Figures 3.7 and 3.8, respectively. The CMC obtained from surface tension measurement is equal to 0.85 mM. For the conductivity measurement, the enhanced counterion binding arising at the very moment that micellization takes place results in a clear break in the conductivity versus concentration plot, indicative of the CMC which is equal to 0.85 mM. Table 3.4 lists the CMC values of CTAB from other literature.

Figure 3.9 shows the viscosity of CTAB as a function of CTAB concentration. The viscosity increase only slightly when the CTAB concentration is increased.

Table 3.4 Literature data on the CMC values of CTAB

T (°C)	CMC (mM)	Methods	References
20	0.85	Surface tension method	Li *et al.*, 1997
25	0.95	Conductivity method	Brackman and Engberts, 1991
a	0.90	*a*	Karlstrom *et al.*, 1990
a	0.93	*a*	Fundin and Brown, 1994

[a] Data not availble

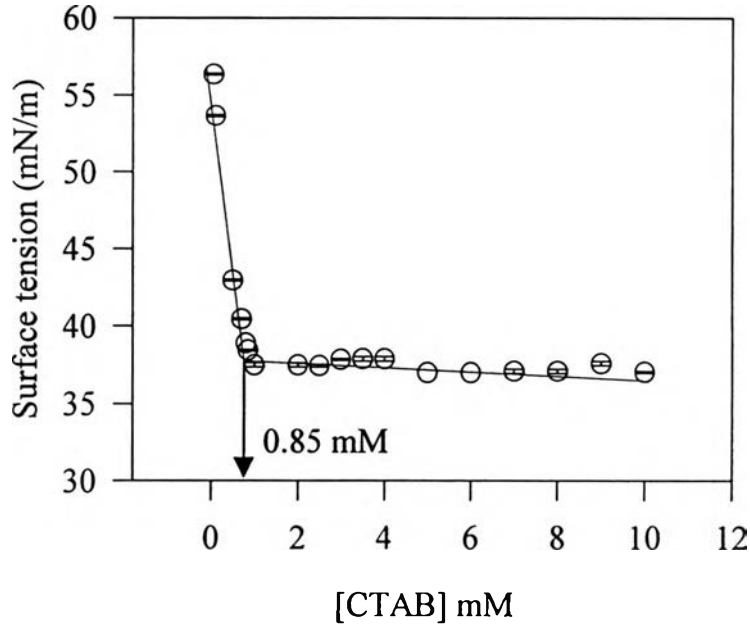

Figure 3.7 Plot of surface tension as a function of total CTAB concentration at 30 °C for the CTAB/water system.

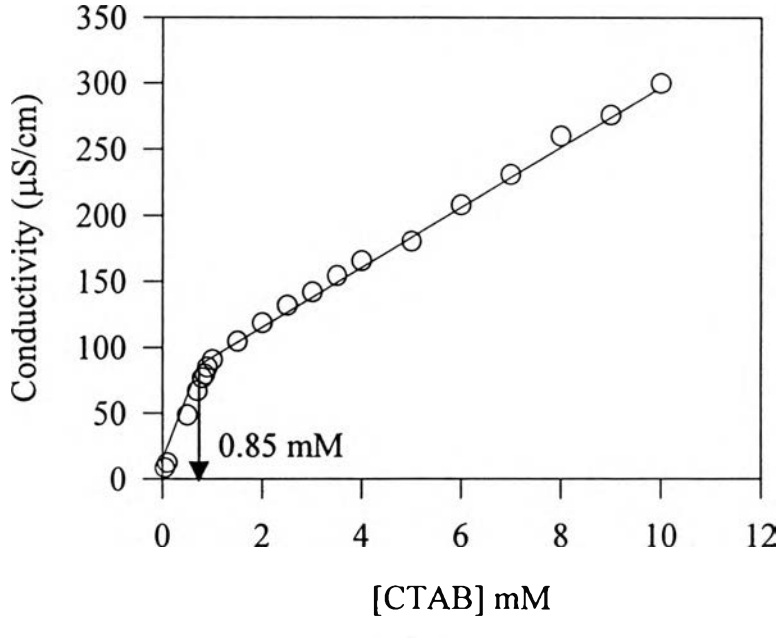

Figure 3.8 Plot of conductivity as a function of total CTAB concentration at 30 °C for the CTAB/water system.

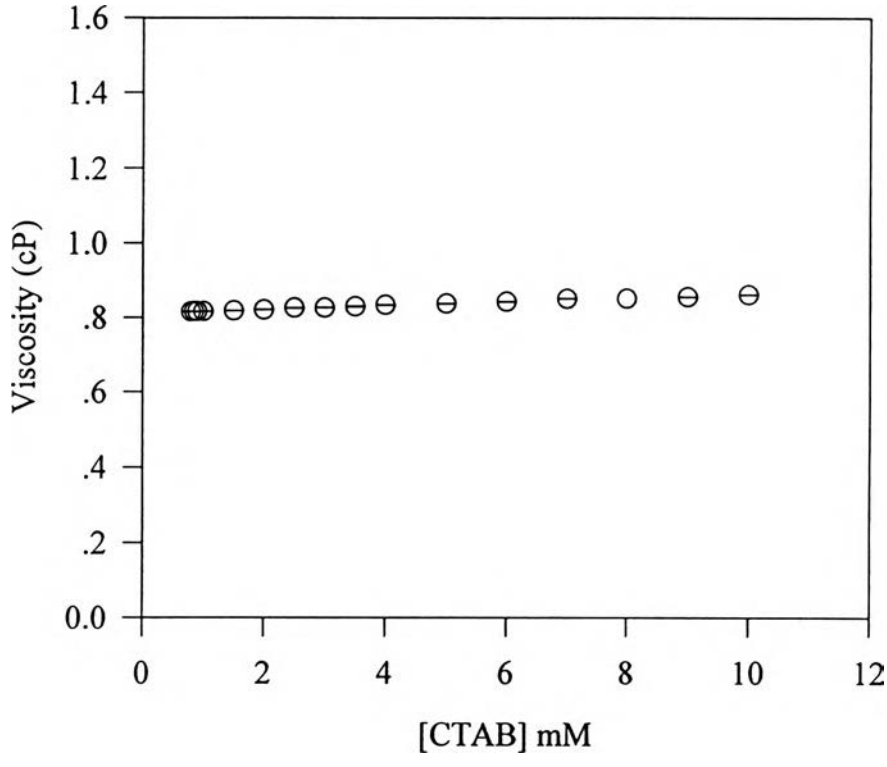

Figure 3.9 Plot of the viscosity as a function of total CTAB concentration at 30 °C for the CTAB/water system.

3.2 Ternary Systems

Several methods such as viscosity, surface tension , conductivity, and dynamic light scattering have been utilized to characterize the interaction between the nonionic water-soluble polymer HPC and the two different types of surfactants, CTAB and OTG. The experiments were performed for selected values of HPC concentrations in the range of 1-5 g/l and for surfactant contents from 0-10 mM for CTAB and 0-63 mM for OTG. All measurements were obtained at 30 °C.

3.2.1 The HPC/OTG/Water System

3.2.1.1 Surface Tension Measurement. Figure 3.10 shows the result from surface tension measurement on the HPC/OTG/water system. It indicates that there is no change in CMC for OTG in the presence of the polymer. Winnik (Winnik, 1990) studied the interaction between HPC and OTG by fluorescence measurement. She also reported that the surfactant has the same CMC in the presence of HPC as it does in aqueous solvent alone.

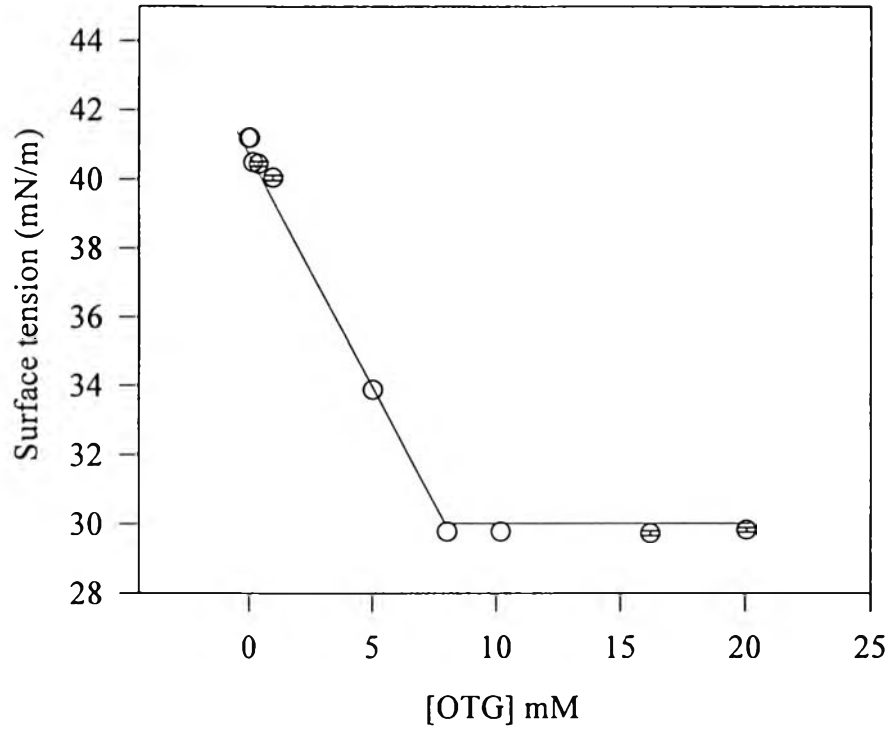

Figure 3.10 Plot of surface tension as a function of total OTG concentration at 30 °C for the HPC/OTG/water system at the fixed HPC concentration of 5 g/l.

3.2.1.2 Viscosity Measurement. Figure 3.11 shows the result from viscosity measurement on the HPC/OTG/water system in term of specific

viscosity; the HPC concentration is constant at 5 g/l while the total OTG concentration was varied. The specific viscosity increases slightly with OTG concentration. For OTG concentration below 20 mM, an increase in the specific viscosity comes directly from the phase volume of OTG molecules or micelles in the system. This situation occurs in the HPC/OTG/water system as well (Figure 3.12).

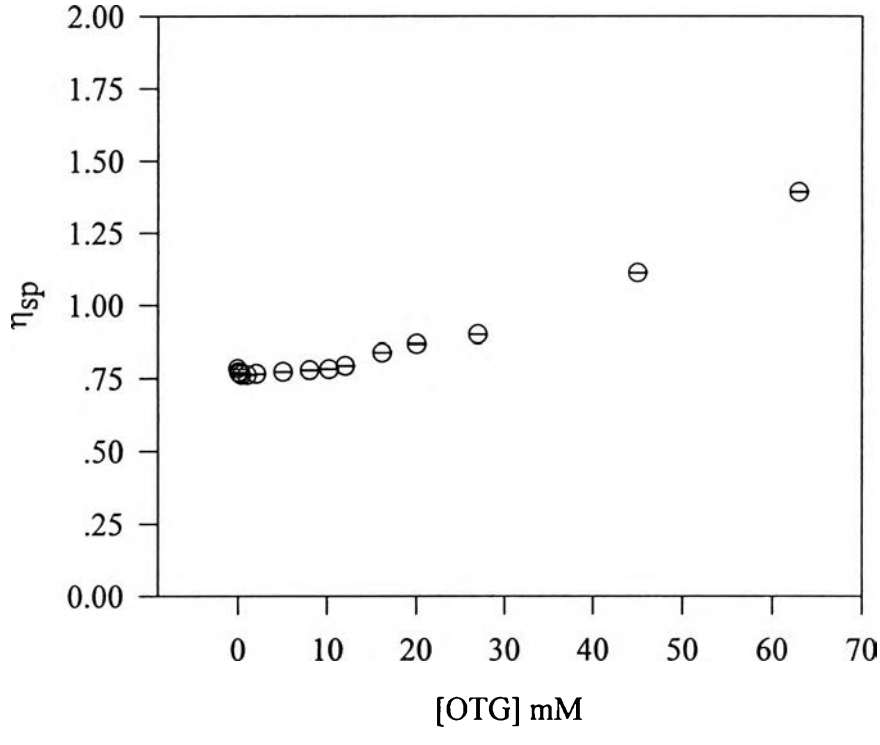

Figure 3.11 Plot of the specific viscosity as a function of total OTG concentration at 30 °C for the HPC/OTG/water system at the fixed HPC concentration of 5 g/l.

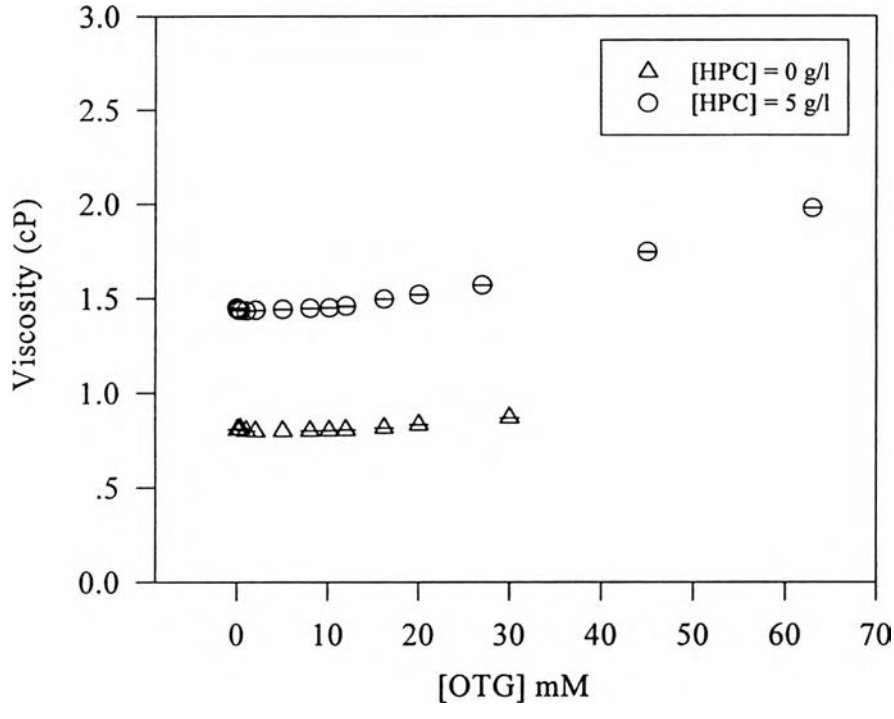

Figure 3.12 Plot of the viscosity as a function of total OTG concentration at 30 °C for the HPC/OTG/water system and the OTG/water system.

3.2.1.3 Dynamic Light Scattering Measurement. Figures 3.13 and 3.14 show the diffusion coefficient and the hydrodynamic radius as a function of OTG concentration for the HPC/OTG/water system. The HPC concentration was fixed at 5 g/l. The apparent hydrodynamic radius is independent of OTG concentration suggesting that no interaction occurs..

Brackman *et al.* (Brackman *et al.*, 1990) studied the possible complex formation of the water-soluble nonionic polymers PEO, PPO, PVP, PVA-PVAc, and HPC with the nonionic surfactant OTG. Only for the PPO/OTG/water system was Brackman *et al.* able to detect the polymer-surfactant complex by microcalorimetry and turbidity measurements. However,

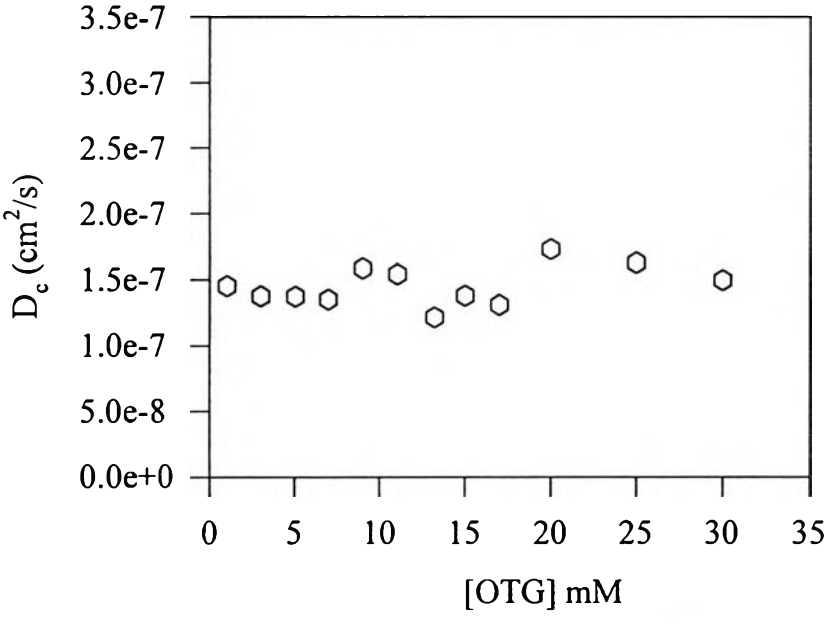

Figure 3.13 Plot of the diffusion coefficient as a function of total OTG concentration at 30 °C for the HPC/OTG/water system at the fixed HPC concentration of 5 g/l.

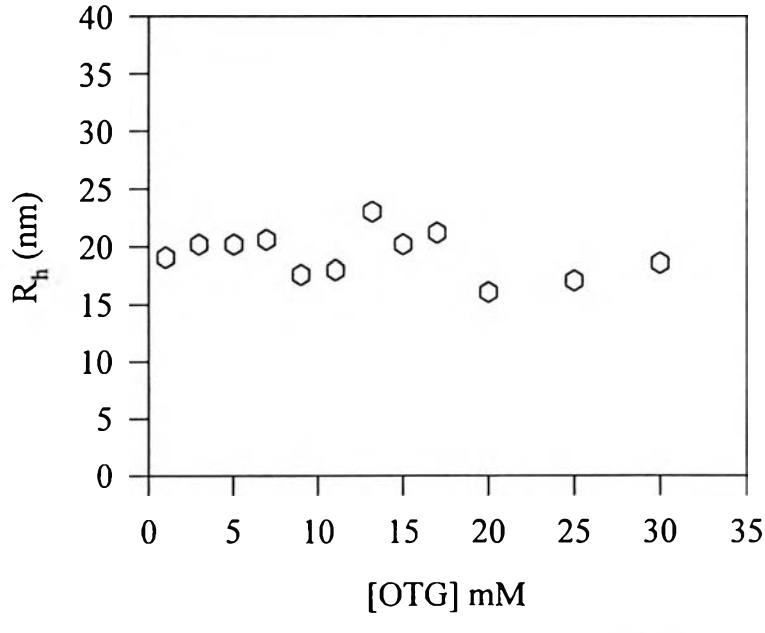

Figure 3.14 Plot of the hydrodynamic radius as a function of total OTG concentration at 30 °C for the HPC/OTG/water system at the fixed HPC concentration of 5 g/l.

for the HPC/OTG/water system, Winnik (Winnik, 1990) reported an evidence for the formation of complexes between HPC and OTG. This evidence came from experiments with a pyrene-labeled (hydroxypropylcellulose) (HPC/Py). We therefore cannot unambiguously conclude from our results that there is no interaction between HPC and OTG. Possibly, the binding of nonionic surfactant micelle to the polymer chain does not cause a change in polymer conformation sufficiently large to be detected by dynamic light scattering and viscosity measurements.

3.2.2 The HPC/CTAB/Water System

3.2.2.1 Surface Tension Measurement. Figure 3.15 (a) and 3.15 (b) show plots of surface tension as a function of CTAB concentration for the HPC/CTAB/water system and for fixed HPC concentrations at 1 g/l and 5 g/l, respectively. Both plots show two transition concentrations labelled T_1 and T_2. This suggests that the binding of surfactant molecules with polymer starts at T_1 and continues up to T_2. Beyond T_2 the surface tension is close to that of a solution containing regular surfactant micelle. Thus, T_2 represents the concentration at which there is saturation of the polymer sites with surfactant micelles. The first breakpoint (T_1) is independent of polymer concentration while the second breakpoint (T_2) increases with polymer concentration (Table 3.5).

Table 3.5 T_1 and T_2 for the HPC/CTAB/water system

[HPC] (g/l)	T_1 (mM)	T_2 (mM)
1.	0.85	3.5
5	0.85	4.0

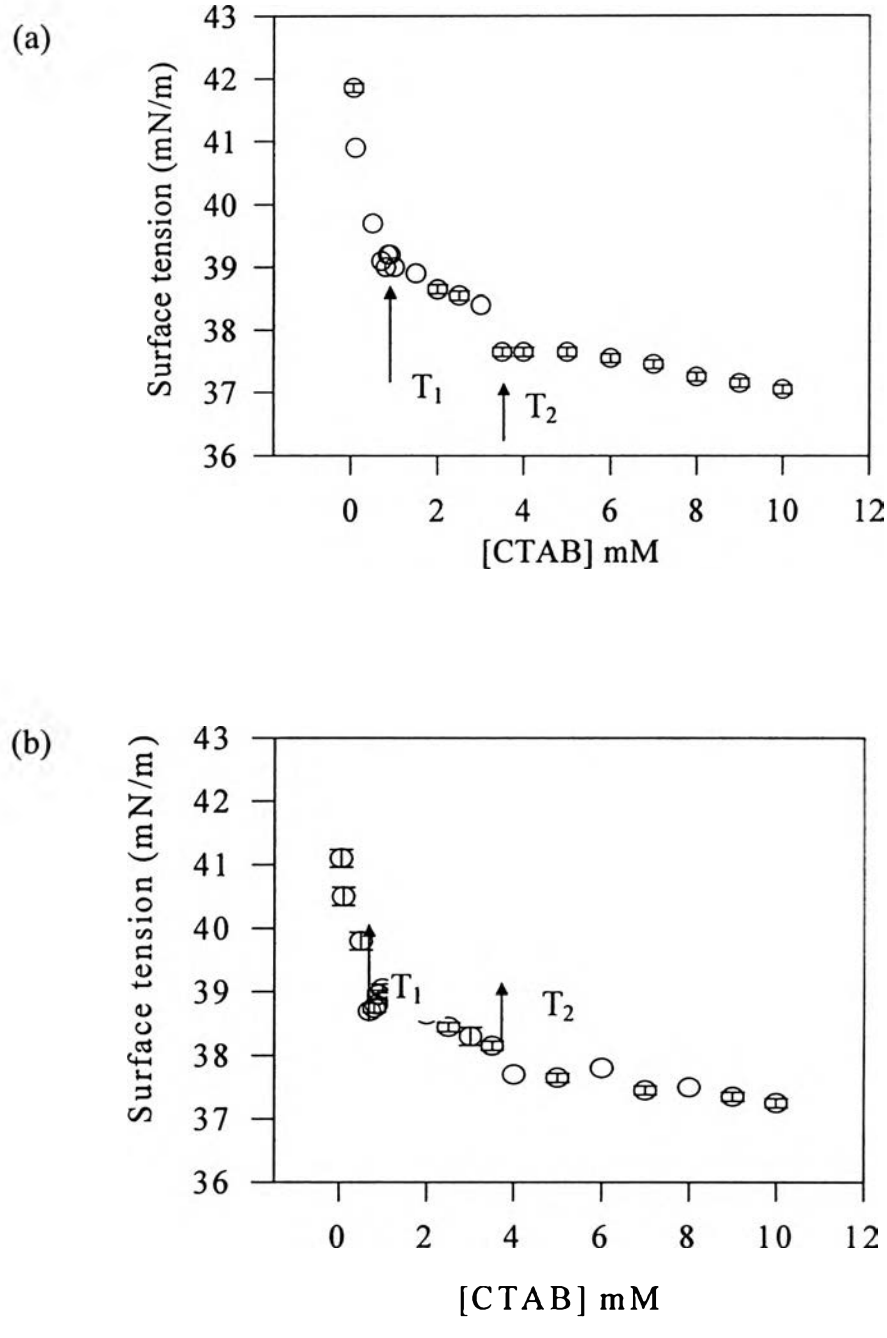

Figure 3.15 Plot of surface tension as a function of total CTAB concentration at 30 °C for the HPC/CTAB/water system and for different HPC concentrations (a) HPC concentration is 1 g/l; (b) HPC concentration is 5 g/l.

3.2.2.3 Conductivity Measurement. Figure 3.16 shows the plot of conductivity as a function of CTAB concentration for the HPC/CTAB/water system at different HPC concentrations at 1 g/l and 5 g/l. The plot shows that a sharp breakpoint for each system occurs at the same CTAB concentration T_1 which is equal to 0.85 mM. The T_2 transition is not involved in the conductivity measurements.

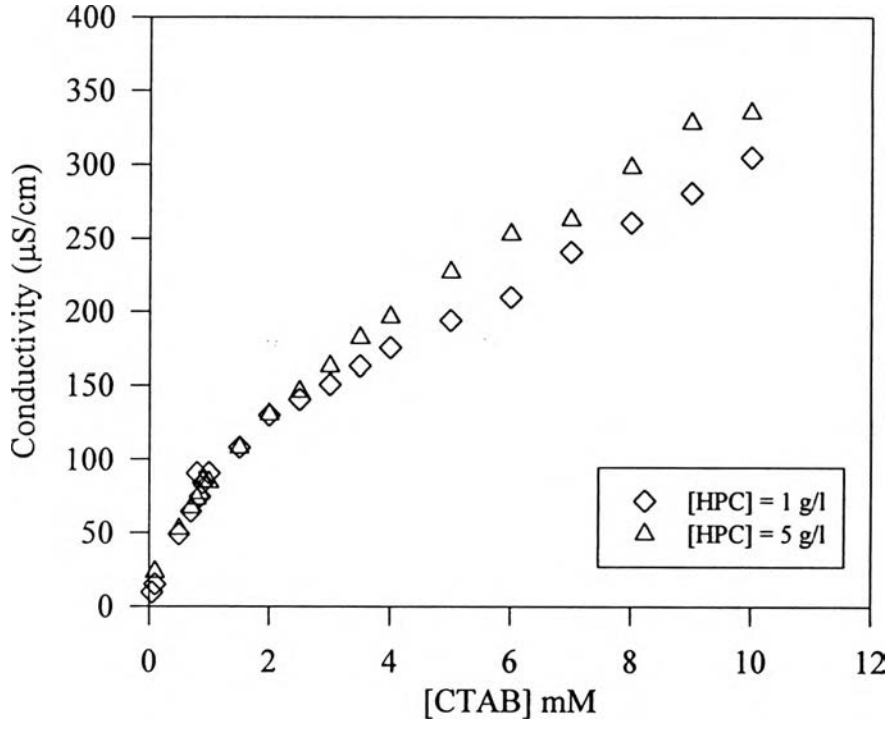

Figure 3.16 Plot of conductivity as a function of the total CTAB concentration at 30 °C for the HPC/CTAB/water system at different HPC concentrations as shown.

3.2.2.4 Viscosity Measurement. Complexes form polymers and ionic surfactants are expected to show changes in their size and shape which depend on the ionic strength, since their physicochemical behavior will be similar to that of a polyelectrolyte. A study of the viscosity and diffusion behavior of such solutions can confirm this point.

(a) Effect of Surfactant Concentration

Figure 3.17 shows the result from viscosity measurements of the HPC/CTAB/water system where the HPC concentration was kept constant at 4 g/l while CTAB concentration was varied.

At low CTAB concentration, an increase in the specific viscosity of HPC upon addition of CTAB to the system occurs presumably because the electrostatic repulsion between the cationic micelles bound to the polymer causes the coil to expand. The specific viscosity of the solution increases until the polymer chains are fully saturated with CTAB, and any further addition of the surfactant to the solution simply adds non-binding micelles to the solution. The decrease of the specific viscosity after the binding saturation concentration can be interpreted in terms of a contraction of the extended coils because of a decrease in the electrostatic repulsion between charge particles due to higher ionic strength of the solution, i.e. the electrostatic screening effect (see Figure 18 (i)). This type of interaction has been observed in other systems such as the HPMC/SDS/water system (Nilsson, 1995), the PEO/SDS/water system (Brown *et al.*, 1992), and the EHEC/SDS/water system (Holmberg *et al.*, 1992) and the hydrophobically end-capped PEO/$C_{12}E_8$/water system (Alami *et al.*, 1996). One must also consider the possibility that intermolecular cross-linking of HPC chains can occur on binding of micelles, and that, above the saturation concentration, the number of cross-links per chain will decrease (see Figure 3.8 (ii)).

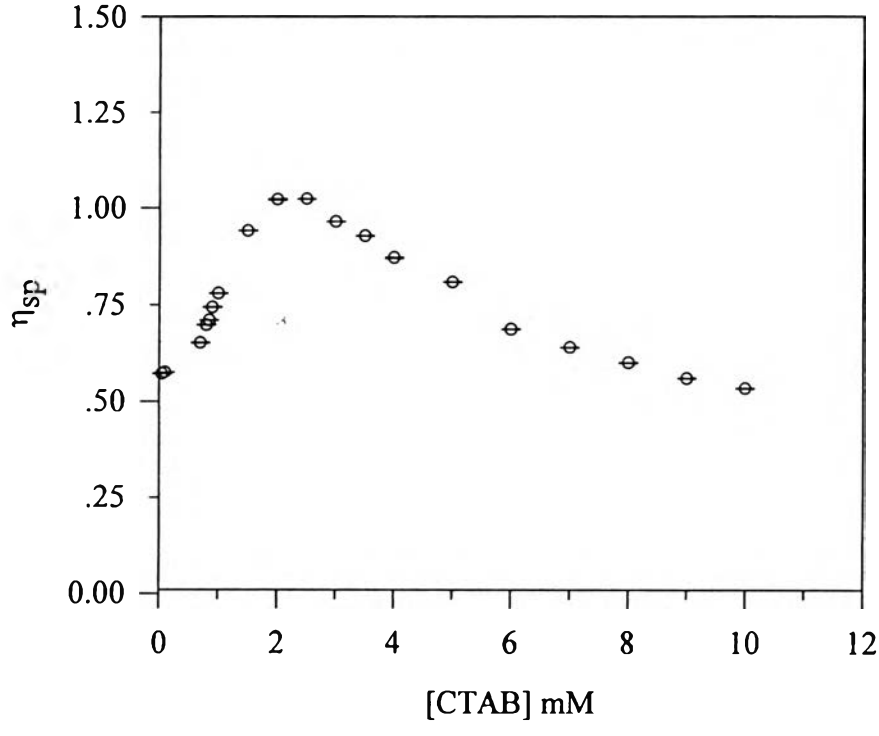

Figure 3.17 Plot of the specific viscosity as a function of total CTAB concentration at 30 °C for the HPC/CTAB/water system at the fixed HPC concentration of 4 g/l.

(b) Effect of Salt

Figure 3.19 shows the effect of salt (NaCl) in the HPC/CTAB/water system where the HPC concentration was fixed at 4 g/l. The ionic strength of the solution can be altered by adding salt into the solution. From this figure, we deduce a decrease in the level of chain expansion induced by complex formation and the level of chain contraction as more salt is added into the solution.

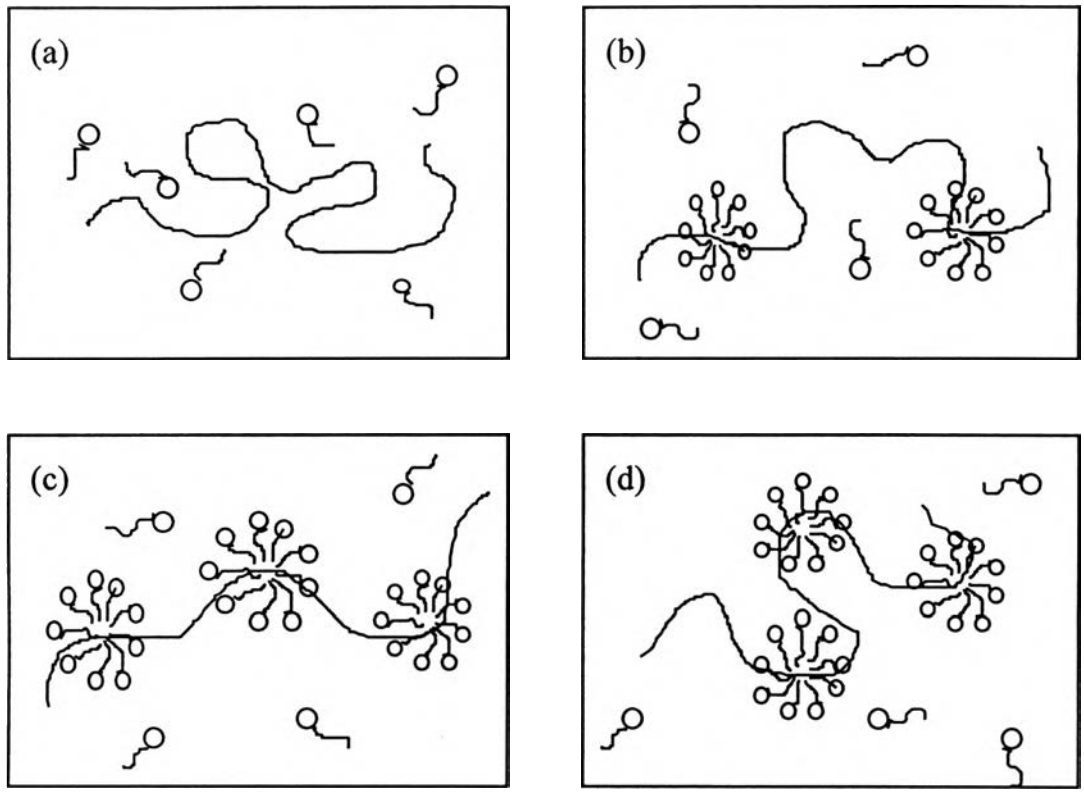

Figure 3.18 (i) Schematic representation of the model proposed for the interaction between HPC and CTAB

(a) At low CTAB concentration, there is no adsorption of CTAB to the HPC chain so there is no change in HPC conformation;

(b) CTAB starts to bind as a cluster to the HPC chain. The polymer-bound CTAB clusters grow in size as the CTAB concentration is increased;

(c) At the binding saturation concentration, the polymer-bound CTAB clusters attain the maximum size due to the electrostatic repulsion between the charged micelles;

(d) Above the binding saturation concentration, the size of the polymer-bound CTAB cluster decreases due to the screening effect of Br^- counterion.

(a)

(b)

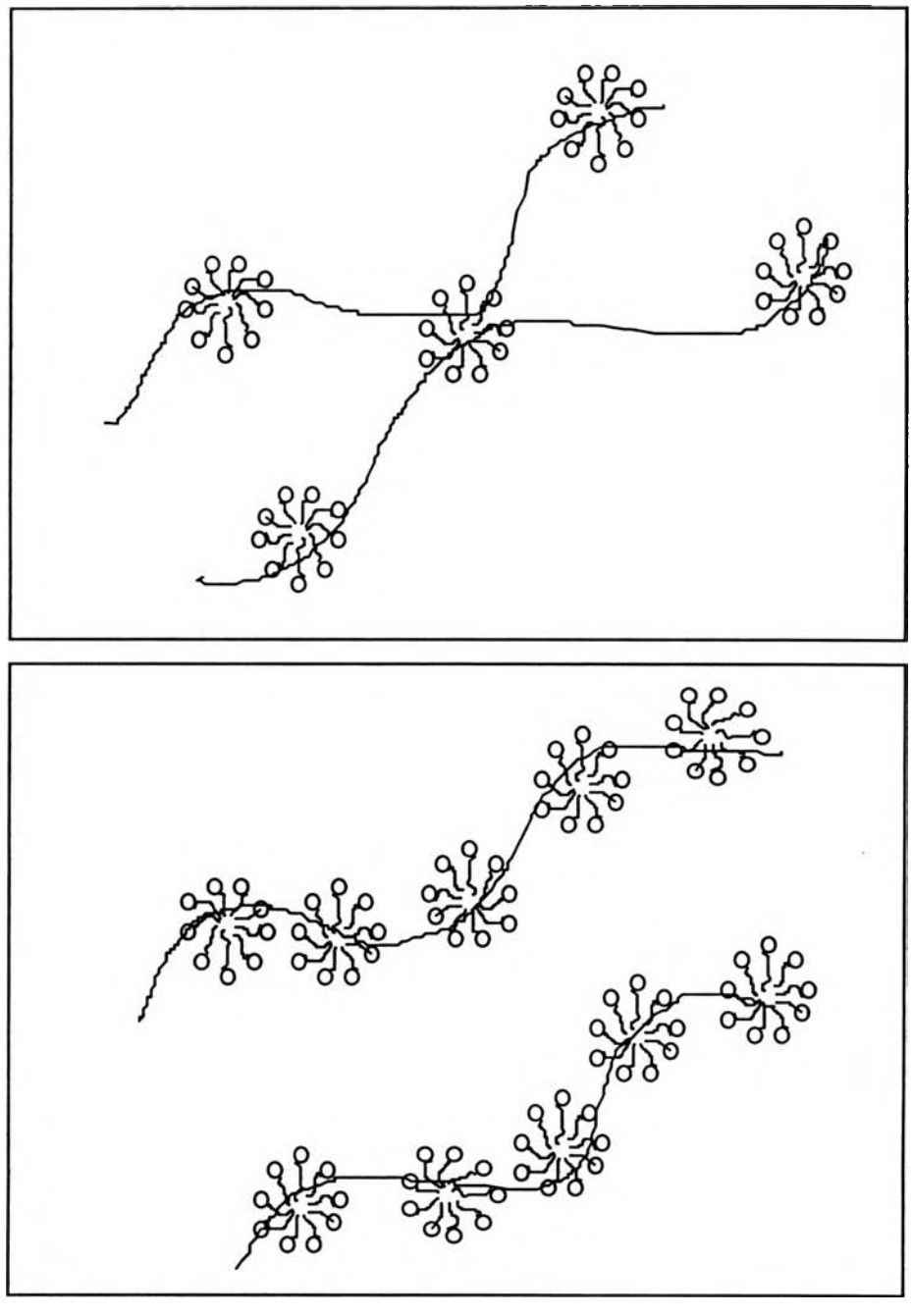

Figure 3.18 (ii) Schematic representation of intermolecular cross-linking of HPC chains by CTAB micelles (a) low CTAB/HPC concentration ratio; (b) high CTAB/HPC concentration ratio.

At lower CTAB concentration, a decrease in the level of chain expansion is due to the effect of Cl^- counterions adsorbed on the Stern layer of bound micelles which shields the repulsion interaction between the charged micelles along the polymer chain. At higher CTAB concentration (after the binding saturation concentration), a decrease in the level of chain contraction is due to the screening effect of free Cl^- counterions. This observation agrees with the results of Brown *et al.* (Brown *et al.*, 1992). They studied the interaction between PEO and SDS and found that there is a slight contraction of PEO coil dimensions as the ionic strength is increased. The maximum in η_{sp} reported by Brown *et al.* is broad on the SDS concentration scale and this is in accord with our present study where the maximum is broad on the CTAB concentration scale.

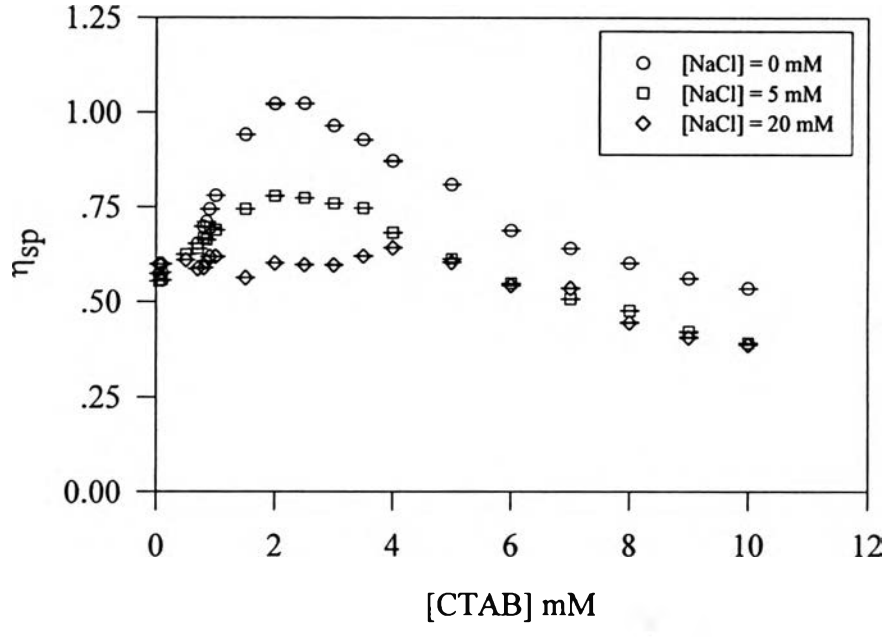

Figure 3.19 Plot of the specific viscosity as a function of total CTAB concentration at 30 °C for the HPC/CTAB/water system at different concentrations of NaCl. The HPC concentration was fixed at 4 g/l.

(c) Effect of Polymer Concentration as a Function of Surfactant Concentration

Figure 3.20 shows the effect of polymer concentration in η_{sp} for the HPC/CTAB/water system. It shows that an increase in the polymer concentration increases proportionally the saturation binding surfactant concentration for this system. The binding saturation concentrations at various HPC concentrations are listed in Table 3.6. Reekmans *et al.*(Reekmans *et al.*, 1993) studied the effect of polymer concentration of the CTAC/PVOH-Ac system and they also reported nearly similar results.

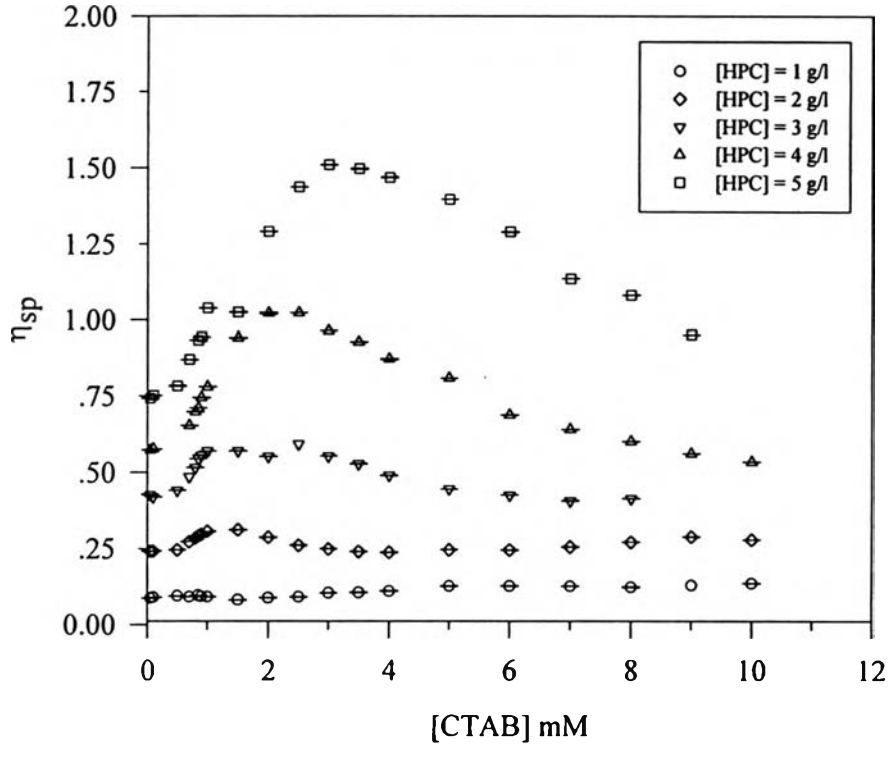

Figure 3.20 Plot of the specific viscosity as a function of total CTAB concentration at 30 °C for the HPC/CTAB/water system at different HPC concentrations.

Table 3.6 The binding saturation concentrations in term of CTAB concentration at various polymer concentrations

[HPC] (g/l)	The saturation concentration ([CTAB], mM)
1	0.5
2	1.0
3	1.5
4	2.0
5	3.0

(d) Effect of Polymer Concentration as a Function of the Surfactant/Polymer Concentration Ratio

Figure 3.21 shows the effect of polymer concentration on η_{sp} in the HPC/CTAB/water system as a function of the CTAB/HPC concentration ratio. At fixed HPC concentration, the specific viscosity increases with the CTAB/HPC concentration ratio until it reaches the saturation concentration. Then the specific viscosity decreases again. This situation can be explained by using the agreements discussed above for the effect of increase in surfactant concentration. For a given CTAB/HPC concentration ratio, the specific viscosity increases with HPC concentration. It is interesting that the binding saturation concentrations for different HPC concentrations occur at approximately the same value of the CTAB/HPC concentration ratio, [CTAB]/ [HPC] = 0.182. The results are summarized in Table 3.7. This suggests that there is a specific molar amount of CTAB bound to each mole of HPC chains.

Table 3.7 The binding saturation concentration in term of the CTAB/HPC concentration ratio at various polymer concentrations

[HPC] (g/l)	The saturation concentration ([CTAB]/[HPC])
1	0.182
2	0.182
3	0.182
4	0.182
5	0.219

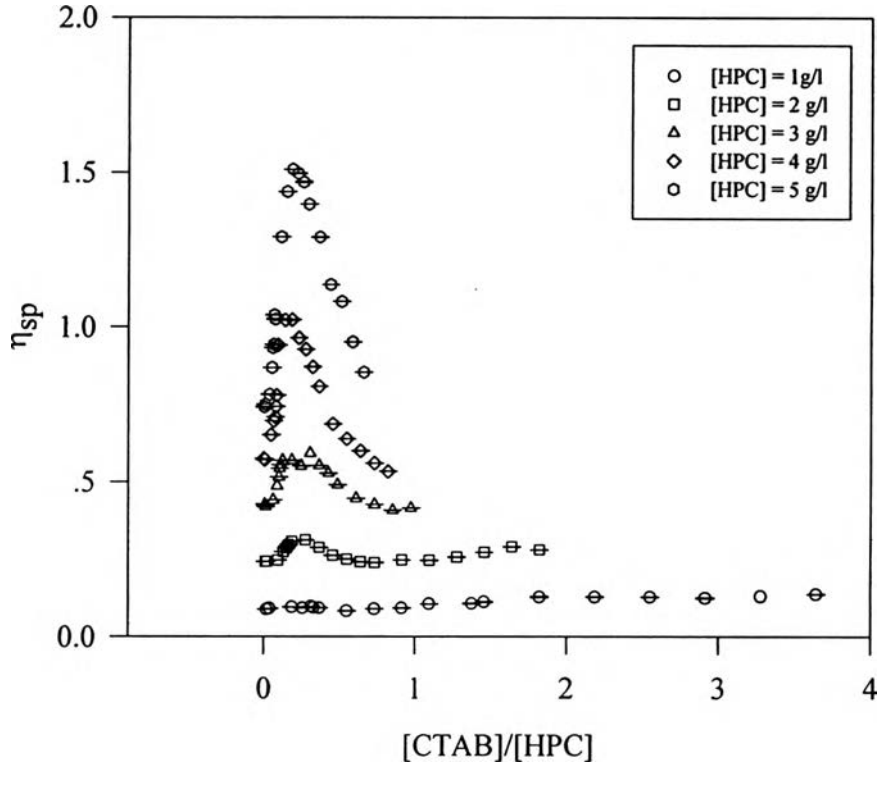

Figure 3.21 Plot of the specific viscosity as a function of the CTAB/HPC concentration ratio at 30 °C for the HPC/CTAB/water system at different HPC concentrations.

For the HPC/CTAB/water system, due to the complex formation between HPC and CTAB, the viscosity of the solution can be expressed as follow:

$$\eta_{solution} = \eta_{polymer} + \eta_{surfactant} + \eta_{solvent} + \eta_{interaction} \quad (3.5)$$

Therefore, the interaction viscosity can be obtained by the subtraction of the solution viscosity from the viscosity of other three terms.

$$\eta_{interaction} = \eta_{solution} - \eta_{polymer} - \eta_{surfactant} - \eta_{solvent} \quad (3.6)$$

Because the surfactant viscosity is very small relative to the solvent viscosity so equation (3.6) can be simplified to

$$\eta_{interaction} = \eta_{solution} - \eta_{polymer} - \eta_{solvent} \quad (3.7)$$

Figure 3.22 shows the plot of the ratio of the interaction viscosity (η_I) to the interaction viscosity at the binding saturation concentration ($\eta_{I, max}$) for the HPC/CTAB/water system at different HPC concentrations. The plot shows that the $\eta_I/\eta_{I, max}$ curves plotted versus [CTAB]/[HPC] ratio approximately collapse into a single curve which can be called "self-similar". The meaning of "self-similar' refers to the contribution of specific viscosity per complex at a given micelles/polymer chain ratio is the same regardless of the number of polymer chains, provided the solution is dilute. We can use this graph for prediction the interaction viscosity in the dilute regime for the HPC/CTAB/water system.

Theoretically, the solution viscosity can be defined as the equation (3.8).

$$\eta_{solution} = \eta_{solvent}(1+2.5\phi_{HPC} + 2.5\phi_{CTAB} + 2.5\phi_{Complex}) \quad (3.8)$$

Assume that there is no free HPC chains and nonbound micelles so equation (3.8) can be simplified to

$$\eta_{solution} = \eta_{solvent}(1 + 2.5\phi_{Complex}) \quad (3.9)$$
$$= \eta_{solvent} + \eta_{solvent}[2.5\times (N_A V_{complex})/M_{complex}]c_{complex}$$

Threfore, we have

$$\eta_{interaction} = \eta_{solvent}[2.5\times (N_A V_{complex})/M_{complex}]\, c_{complex} \quad (3.10)$$

The reason for the increase in interaction viscosity although the molecular weight of complex increases is because the increase in hydrodynamic volume due to the electrostatic interaction has a greater effect than the increase in the molecular weight of complex. At the saturation concentration, the molecular weight of complex is constant so the interaction viscosity decreases because the hydrodynamic volume decreases due to the screening effect.

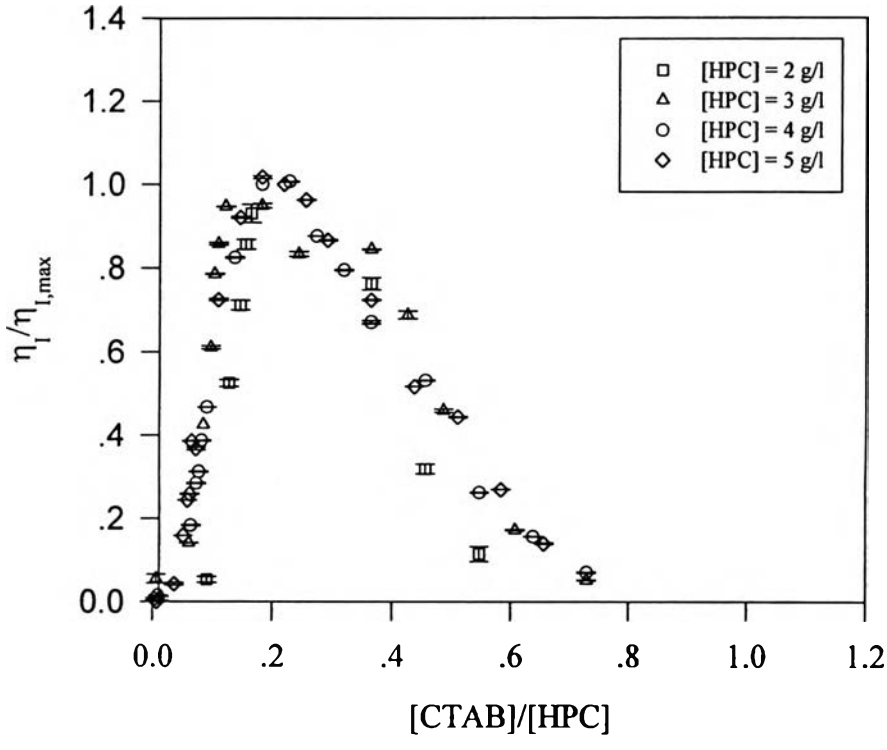

Figure 3.22 Plot of $\eta_I/\eta_{I,\,max}$ as a function of the CTAB/HPC concentration ratio at 30 °C for the HPC/CTAB/water system at different HPC concentrations.

3.2.2.5 Dynamic Light Scattering Measurement. Dynamic light scattering measurements were made on mixtures of HPC and CTAB in dilute solution regime. All measurements were made at 30 °C.

(a) Effect of Surfactant Concentration

Figure 3.23 shows the mean translational diffusion coefficient as a function of CTAB concentration for the HPC/CTAB/water system at 5 g/l HPC. At low surfactant concentration, the diffusion coefficient decreases strongly until it reaches a minimum, indicating the complex formation occurs. After this point, the diffusion coefficient increases with

CTAB concentration again. The hydrodynamic radius of the complex for this system can be calculated by using the Stokes-Einstein equation as shown in Figure 3.24. This result agrees with the result of the viscosity measurement. At low addition of surfactant to the polymer solution, the complex starts to form, resulting in an increase of both hydrodynamic radius and viscosity. After the saturated concentration, the hydrodynamic radius decrease in the same trend of viscosity due to the screening effect of Br^- counterion.

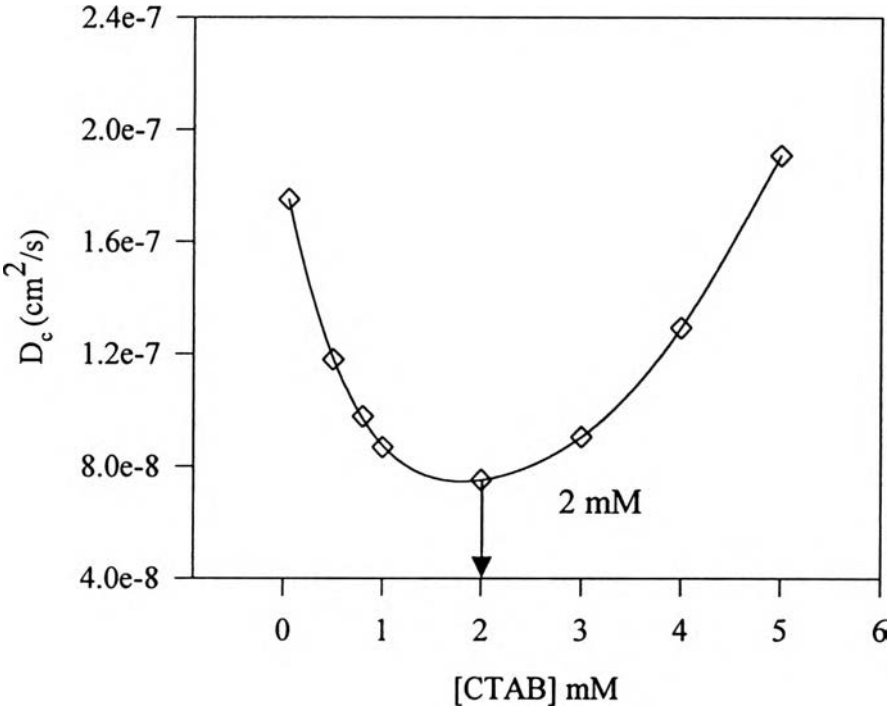

Figure 3.23 Plot of the diffusion coefficient as a function of total CTAB concentration at 30 °C for the HPC/CTAB/water system at the fixed HPC concentration of 5 g/l.

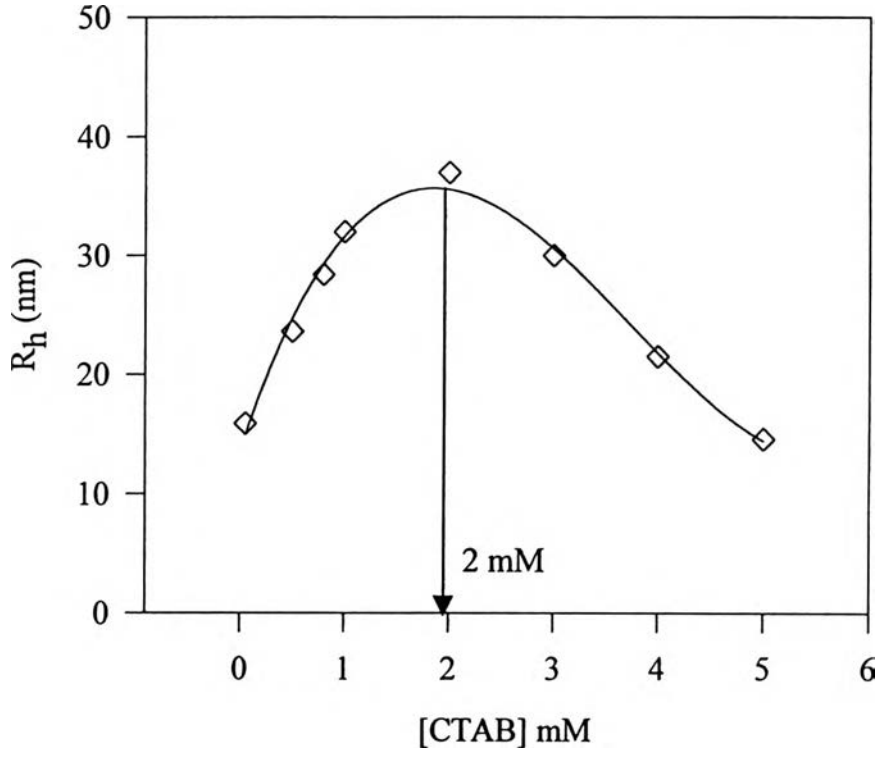

Figure 3.24 Plot of the hydrodynamic radius as a function of total CTAB concentration at 30 °C for the HPC/CTAB/water system and for the fixed HPC concentration of 5 g/l.

(b) Effect of Polymer Concentration as a Function of Surfactant Concentration

Figures 3.25 and 3.26 show the effect of polymer concentration for the HPC/CTAB/water system and for different HPC concentrations at 1 g/l and 3 g/l, respectively. The results show that the saturated concentration shifts to a higher surfactant concentration when the polymer concentration is increased (Table 3.8). This situation corresponds with the results from the viscosity measurement as discussed previously. A similar result was obtained for the hydrophobically end-capped PEO/$C_{12}E_8$/water system (Alami, *et al.*, 1996).

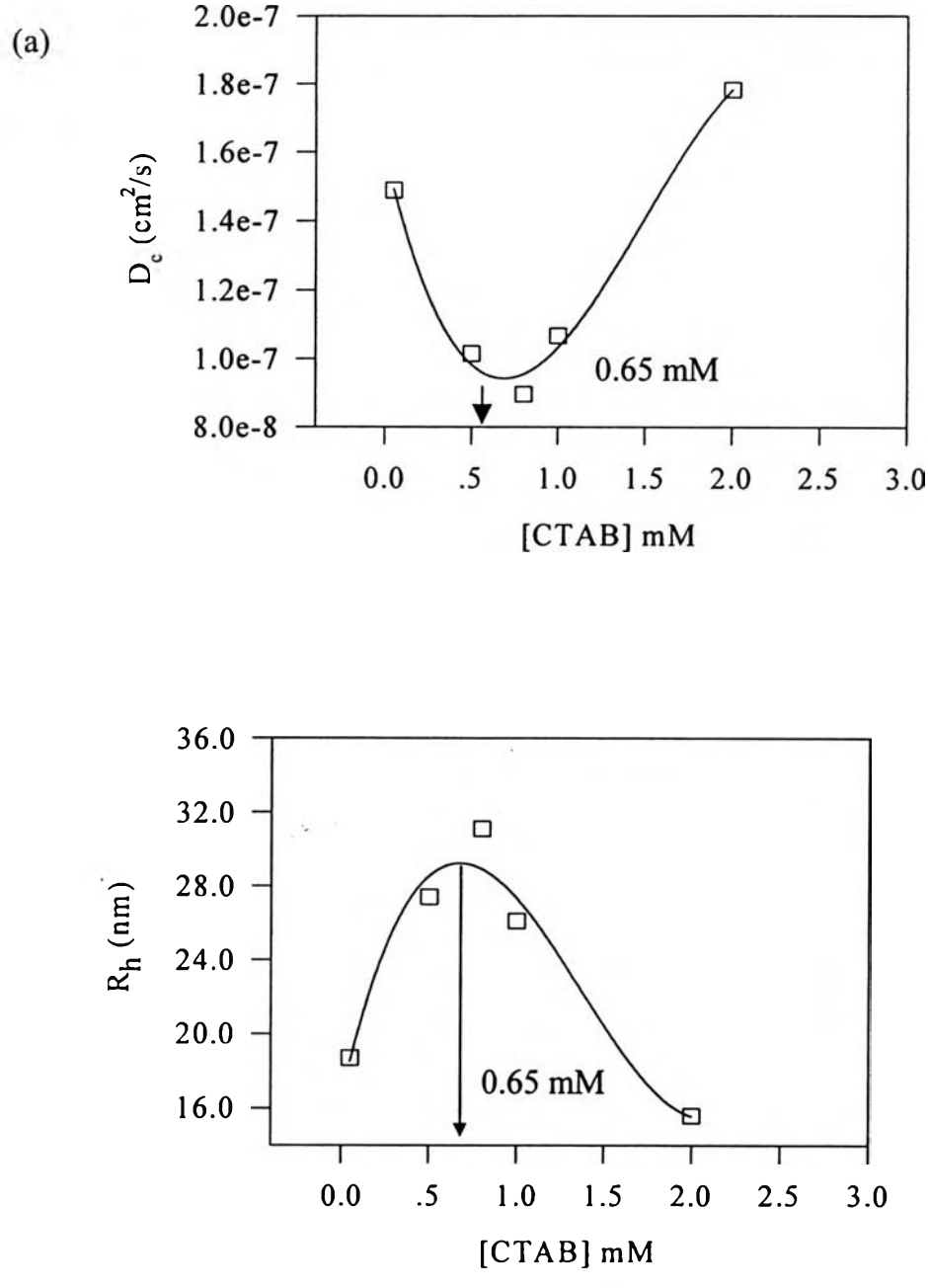

Figure 3.25 Plot of the diffusion coefficient (a) and the hydrodynamic radius (b) as a function of total CTAB concentration at 30 ° C for the HPC/CTAB/water system at the fixed HPC concentration of 1 g/l.

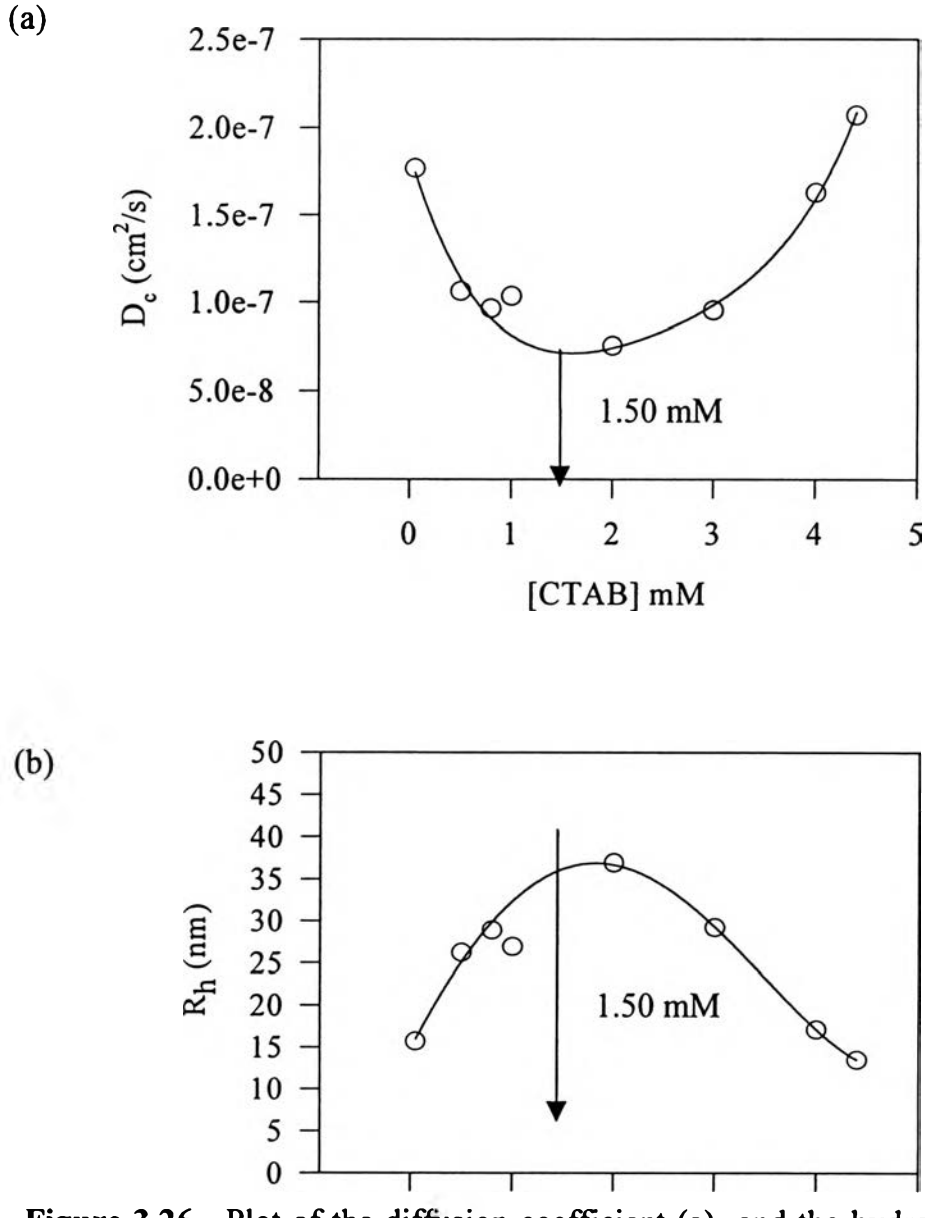

Figure 3.26 Plot of the diffusion coefficient (a) and the hydrodynamic radius (b) as a function of total CTAB concentration at 30 °C for the HPC/CTAB/water system at the fixed HPC concentration of 3 g/l.

Table 3.8 The binding saturation concentration in term of the CTAB concentration at various polymer concentrations

[HPC] (g/l)	The saturation concentration ([CTAB], mM)
1	0.65
3	1.50
5	2.00